Application of a Variational Method for Generating Adaptive Grids

R. I. Kreis*
North Carolina State University, Raleigh, North Carolina
F. C. Thames†
NASA Langley Research Center, Hampton, Virginia
and
H. A. Hassan‡
North Carolina State University, Raleigh, North Carolina

Application of variational methods for generating adaptive grids is not as straightforward as one is led to believe. Proper scaling, suitable weight functions, and appropriate clustering on boundaries must be employed to obtain a satisfactory grid. This work, which is based on the framework developed by Brackbill and Saltzman, provides simple methods for determining scaling and investigates possible options for selecting the weight function and clustering points on the boundaries. The concepts developed here are applied to 2 two-dimensional problems: a model problem based on Burger's equation containing two length scales and transonic flow past airfoils using the Euler equations.

Introduction

IT is generally believed that it takes more than an efficient algorithm to obtain an accurate solution of a complex problem. The grid employed can have a profound influence on the quality and the convergence rate of the solution. Moreover, with the limited storage capabilities of available computers, it is imperative that one concentrates grid points where needed to obtain an accurate solution. This can be achieved by employing adaptive grids.

An adaptive grid is a grid that controls the placement of grid points automatically based on the solution of the physical problem under consideration. An objective of such an adaptation is the minimization of error by the equidistribution of some property of the solution. There are a number of methods for attaining such an objective. Most of these methods can be derived from variational principles[1,2] which, in turn, lead to Euler's variational equations. We selected the method of Brackbill and Saltzman[3] for further investigation because of its conceptual simplicity and because it can accommodate problems characterized by a number of length scales. In addition, it can be extended with little difficulty to three-dimensional grids. The method considers three aspects that are desirable in a mesh: global smoothness, orthogonality, and grid cell size variation. This last quality is responsible for clustering mesh points where needed to more accurately resolve some quantity in the solution.

The objective of this work is not to concentrate on a given problem and generate the best grid the variational method of Ref. 3 can produce. It is much broader than that. When one employs a variational method of the type considered here, one must address important questions pertaining to scaling, weight function selection, and clustering of points on the boundary. Failure to heed any of the above will defeat the purpose of adaptation. The above questions are discussed in conjunction with two problems representative of viscous and inviscid flows. The first involves a solution of the two-dimensional Burger's equation for some difficult boundary conditions that result in a shock wave and a boundary layer.[4] The second involves the solution of the Euler equations of gasdynamics for transonic flows past airfoils. The algorithm employed is that developed by Jameson et al.[5]

Received Nov. 19, 1984; presented as Paper 85-0487 at the AIAA 23rd Aerospace Sciences Meeting, Reno, NV, Jan. 14-17, 1985; revision received June 3, 1985.

*Research Assistant, Mechanical and Aerospace Engineering. Student Member AIAA.
†Aero-Space Technologist, Theoretical Aerodynamic Branch, Transonic Aerodynamics Divison.
‡Professor, Mechanical and Aerospace Engineering. Associate Fellow AIAA.

Analysis

Problem Formulation

As was indicated above, the method of Ref. 3 considers three desirable qualities in a grid: smoothness, orthogonality, and cell size variation. If x,y represent the coordinate in the physical plane and ξ,η the coordinates in the computational plane, then the quantity $(\nabla\xi)^2+(\nabla\eta)^2$ represents the variation of ξ,η over the field or a measure of the roughness of the field. Thus, a smooth grid is one resulting from minimizing the integral

$$I_s=\int[(\nabla\xi)^2+(\nabla\eta)^2]\,dxdy \tag{1}$$

In a similar manner the quantity $\nabla\xi\cdot\nabla\eta$ is zero for an orthogonal grid, and thus, is a measure of departure from orthogonality. Therefore, to minimize departure from orthogonality, one must minimize the integral

$$I_0=\int(\nabla\xi\cdot\nabla\eta)^2J^3\,dxdy \tag{2}$$

where J is the Jacobian of transformation

$$J=\frac{\partial(x,y)}{\partial(\xi,\eta)}=x_\xi y_\eta-x_\eta y_\xi \tag{3}$$

If one wants to concentrate small cells where a strictly positive weight function w is large, then one would like the product of the cell area and the weight function to be con-

stant. This can be obtained by minimizing the integral

$$I_v = \int w J \mathrm{d}x\mathrm{d}y \tag{4}$$

Finally, if it is desired that the grid has all of the above aspects, then a weighted sum I of the above integrals, i.e.,

$$I = I_s + \lambda_v I_v + \lambda_0 I_0 \tag{5}$$

must be minimized. In this work both λ_v and λ_0 are chosen constants.

The grid is generated by solving the Euler equations associated with minimizing the integral indicated in Eq. (5). These equations (2 in two dimensions, 3 in three dimensions) are given in Appendix A. They are, in general a quasilinear coupled system of elliptic equations. Their solution depends on boundary geometry and conditions, λ_0, λ_v and the weight function w. Thus, use of variational techniques for grid adaptation requires the user to specify λ_0, λ_v, w and the manner in which boundary points should be allowed to move.

Minimization of I_s alone gives the "smoothest" possible grid; minimization of I_0 alone results in the most "globally orthogonal" grid, while minimizing I_v alone yields a grid with the desired volume variation as specified by the weight function w. If $J, w > 0$, then the solution of the volume variation part of mesh generator is[3]

$$wJ^2 = \text{const} \tag{6}$$

This fact can be used to determine the extent to which a given mesh has adapted. The quantity wJ^2 will be referred to as the adaptivity product.

Scaling

Because the orthogonality and volume control constants λ_0 and λ_v must be specified a priori, and because it is desirable to control the relative measure of the three grid characteristics, a scaling analysis must be performed to establish the magnitudes of the three integrals. The need for such an analysis becomes evident upon examination of the character of the Euler equations that result from minimizing I_s, I_v, and I_0 individually. These are elliptic, degenerate, and of mixed type, respectively. Thus, if λ_v and λ_0 are chosen at random, the resulting problem may be ill posed and a solution will not be possible. On the other hand, if λ_v and λ_0 are too small, little adaptation and orthogonality control will result.

The first type of scaling that should be performed is global. The Jacobian is implicitly embedded in the transformation, yet its magnitude is arbitrary. Thus, the global scaling analysis will be based on J. Hence, for two dimensions,

$$J = x_\xi y_\eta - x_\eta y_\xi = 0\left(\frac{\Delta x}{\Delta \xi}\frac{\Delta y}{\Delta \eta}\right) = 0\left(\frac{\Delta x}{\Delta \xi}\right)^2 \equiv 0(h^2) \tag{7}$$

The integrands of I_s, I_v, and I_0 are easily shown to be of order

$$1, wh^4, h^4 \tag{8}$$

If w is chosen to be of order 1, then λ_v and λ_0 must be chosen so that

$$\lambda_v = \beta_v / h^4, \quad \lambda_0 = \beta_0 / h^4 \tag{9}$$

with β_v and β_0 of order 1-10. The above choice insures that all components of i are of the same order.

The above scaling by itself is inappropriate when J changes by several orders of magnitude as is the case for applications involving nearly "unbounded" domains (e.g., flows past airfoils). For example, solutions based on the potential equation or the Euler equations employ grids where the ratio of $J_{\max}$ to $J_{\min}$ can exceed 10^6. Because the weight function normally has a limited range and because the grid is trying to adapt according to Eq. (6), the solution will attempt to make $J^2 \approx$ const. Thus, instead of clustering points close to the airfoil surface, the above procedure ends up doing the opposite.

The solution to this problem can be deduced from Eq. (8). Rather than requiring w to be of order 1, one should require wJ^2 to be of order 1. This indicates a choice of w of the type

$$w(x,y) \sim (\nabla f)^2 \tag{10}$$

where f is a solution property selected by the user. Upon transformation, Eq. (10) can be written as

$$w = w_0(\xi,\eta)/J^2 \tag{11}$$

with w_0 being of order unity. This choice of w requires a λ_v or order 1. Parameters employed in this work were chosen in such a way as to maintain the elliptic character of the equations governing the grid. Such a choice will prevent overadaptation.

Results and Discussion

There are two approaches for generating adaptive grids for time or pseudo-time-dependent problems. In the first, the grid evolves with the solution at each time step. In the second, the grid is changed only at selected times. In this work grids were changed at selected time or iteration steps. Because of this, interpolation was used to transfer values from the old grid to the new. Based on our experience, the initial grid for the calculation of problems characterized by a number of length scales must be capable of resolving all length scales. Moreover, if the weight function does not reflect the correct physics of the problem, then the grid cannot possibly adapt in a manner that will bring about an accurate solution of the problem. Therefore, adaptation should not start before the solution exhibits the correct physical features of the final solution.

The weight function may be chosen as a first or second derivative (or a combination of both) of a solution property or combination of solution properties. Because of errors associated with numerical differentiation, it may be necessary to smooth the weight function before commencing with the grid calculations. We experimented with first and second derivative-type weight functions. In general, the latter required more smoothing. Based on the results, the extra effort could not be justified. Therefore, all the results presented here employed first derivative weight functions.

Linear Burger's Equation

Global scaling is incorporated into the grid algorithm to obtain the solution of Burger's equation:

$$U_t - U_x + U_y = \epsilon(U_{xx} + U_{yy}) \tag{12}$$

subject to the boundary conditions[4]

$$U(x,0) = U(0,y) = 1, \quad U(x,1) = 0, \quad x > 0$$

$$U(1,y) = \begin{cases} 1, & y \le 0.5 \\ 0, & y > 0.5 \end{cases} \tag{13}$$

The solution to this problem has a "boundary layer" along the $y = 1$ line from $x = 0$ to $x = 0.5$, and a "shock" along the line connecting the points (0.5, 1.0) and (1.0, 0.5). The points on the boundary were allowed to move to insure orthogonality there.

A number of choices of w based on the gradients of U were investigated. To test the concepts developed for global

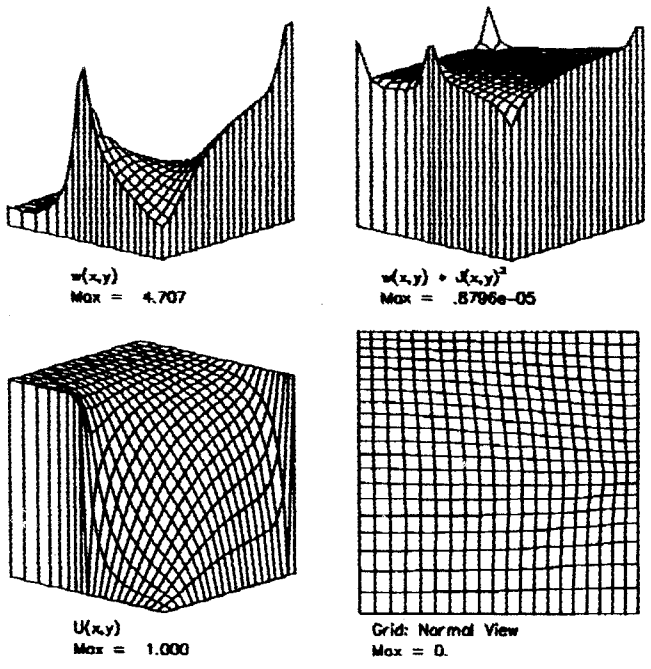

Fig. 1 Solution (U), weight function (w), adaptivity product (wJ^2), and grid normal view for Burger's equation solution ($\epsilon = 0.1$, $\beta_v = 10$, $\beta_0 = 0$).

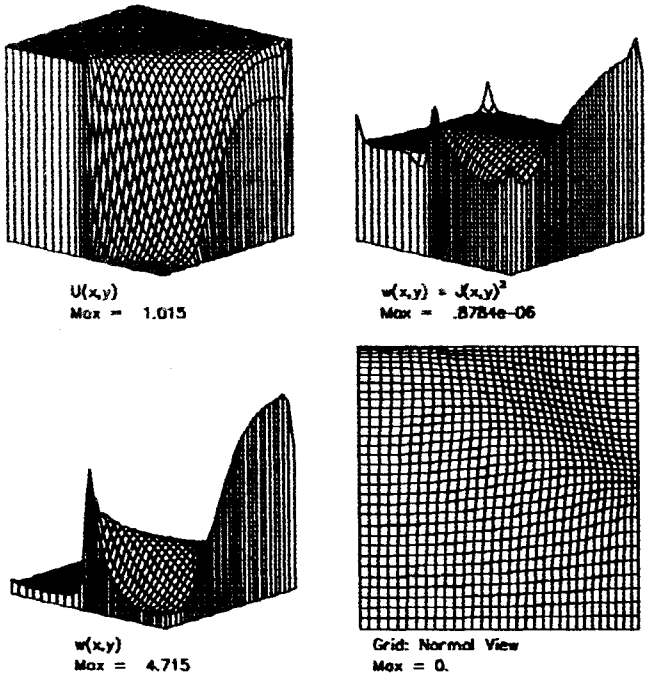

Fig. 2 Solution (U), weight function (w), adaptivity product (wJ^2), and grid normal view for Burger's equation solution ($\epsilon = 0.01$, $\beta_v = 10$, $\beta_0 = 0$).

scaling, the weight function is chosen as

$$w = C_1 |\nabla U|^{\sigma} + C_2 \tag{14}$$

where C_1, C_2, and σ are constants and are chosen so that w is of order 1. Figures 1-3 are based on the above choice with $C_1 = 5$, $C_2 = 0.25$, and $\sigma = 0.5$. In Fig. 1, $\epsilon = 0.1$, $\beta_v = 10$, and $\beta_0 = 0$. In Figs. 2 and 3, $\epsilon = 0.01$, $\beta_v = 10$, and $\beta_0 = 0,1$, respectively. All figures show the solution U, the weight function w, wJ^2, and the resulting grid. As is seen from the figures, clustering is indicated around the shock wave and boundary layer. Moreover, they show that wJ^2 is almost constant, indicating a successful adaptation.

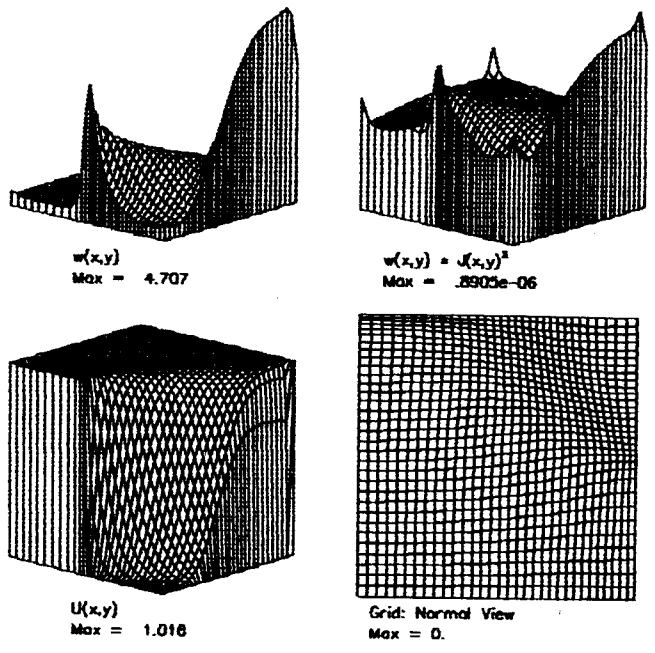

Fig. 3 Solution (U), weight function (w), adaptivity product (wJ^2), and grid normal view for Burger's equation solution ($\epsilon = 0.01$, $\beta_v = 10$, $\beta_0 = 1$).

Table 1 Grids used in FL052 calculations of NACA 0012 airfoil flows

Grid	Type	Boundary point distribution
1	Nonadaptive (standard FL052)	Fixed
2	Nonadaptive ("smooth," $\beta_v = 0$, $\beta_0 = 0$)	Fixed
3	Adaptive ($\beta_v = 10$, $\beta_0 = 0$)	Fixed
4	Adaptive ($\beta_v = 10$, $\beta_0 = 0$)	Grid normal to airfoil surface
5	Adaptive ($\beta_v = 10$, $\beta_0 = 0$)	$(s_i/s_{\max})_{\eta=1} = (s_i/s_{\max})_{\eta=2}$

Transonic Airfoils

Among the schemes for adapting grids in flows past airfoils at transonic Mach numbers, Nakamura[6] determines the weight function from a diffusion-like equation and employs the potential equation to determine the flowfield. On the other hand, the scheme of Steinbrenner et al.[7] employs equidistribution in one coordinate direction, similar to that used by Dwyer[8] and Gnoffo,[9] in conjunction with Euler equations. In this work, the solution algorithm employed is a version of FL052 developed by Jameson et al.,[5] and the weight function employed had the form indicated in Eqs. (10) and (11). The method of solution of the equations that govern the grid is outlined in Appendix A.

In the remainder of this section, comparisons of surface pressure distributions computed by the FL052 code on an NACA 0012 airfoil using five different grids, both adaptive and nonadaptive, will be shown. The free-flight conditions for all runs were the same, namely, $M_\infty = 0.8$ and $\alpha = 0$. The properties of the various grids are summarized in Table 1.

Details of the native grid employed by FL052 for calculating transonic flow on an NACA 0012 airfoil are

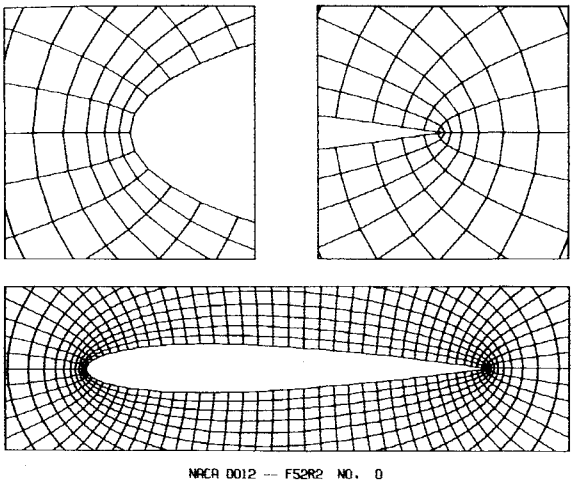

Fig. 4 Selected portions of grid 1.

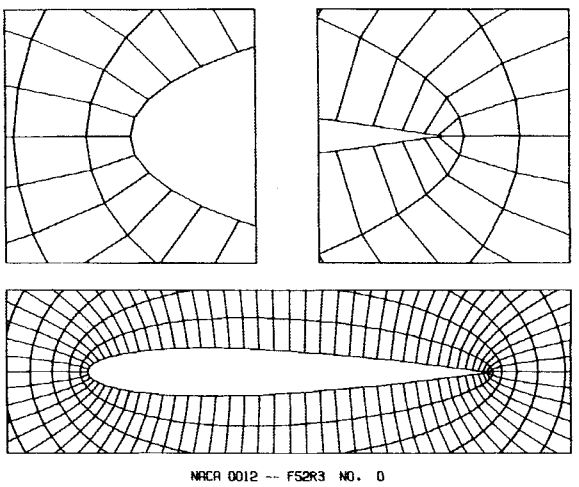

Fig. 5 Selected portions of grid 2.

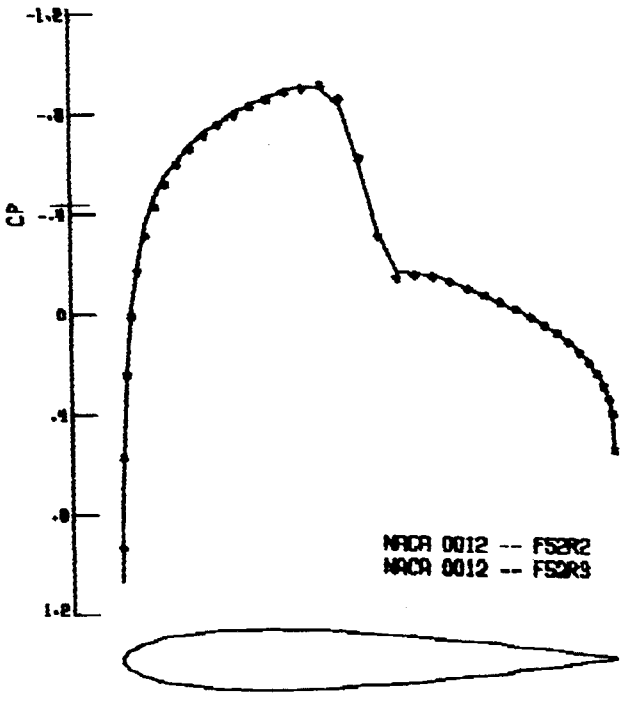

Fig. 6 Pressure distribution comparison: grid 1 (solid line), grid 2 (symbols).

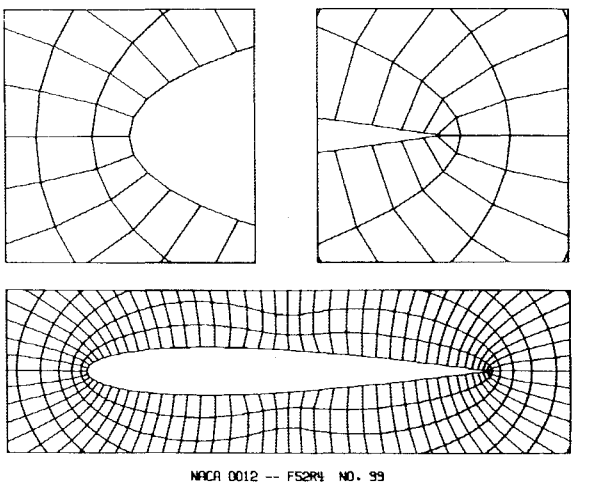

Fig. 7a Selected portions of grid 3.

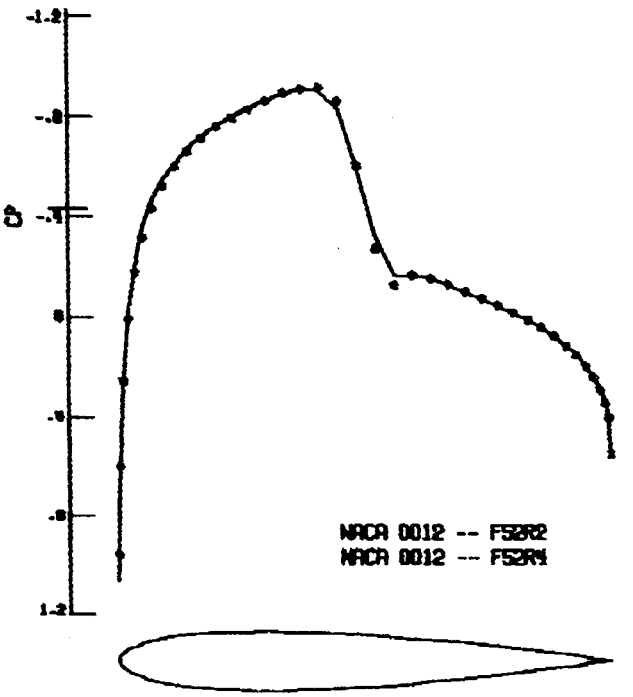

Fig. 7b Pressure distribution comparison: grid 1 (solid line), grid 3 (symbols).

shown in Fig. 4 (grid 1 in Table 1). For the sake of clarity, only the grid in the immediate neighborhood of the airfoil is pictured. Figure 5 gives similar details for grid 2, that is, the "smooth" grid corresponding to $\beta_v = \beta_0 = 0$. Although both grids employ the same number of cells (80×20), grid 1 clusters more points closer to the airfoil surface. Figure 6 compares the pressure distributions computed on grids 1 and 2. The solid line is the solution of FL052 on its "own" grid (i.e., grid 1), while the symbols denote the solution on grid 2. In spite of the differences in the two grids, the two calculations are in good agreement with each other. However, neither calculation resolves the shock well because the grids are somewhat coarse in the region of the shock.

The results given below compare the pressure distributions on grid 1 with those obtained with various adaptive grids (grids 3-5). In all of the adaptive calculations, the quantity f in Eq. (10) is taken to be the pressure. With the weight function w thus specified, the only remaining input for the solution of the adaptive grid problem is a scheme for distributing and moving points on the airfoil boundary. As indicated in

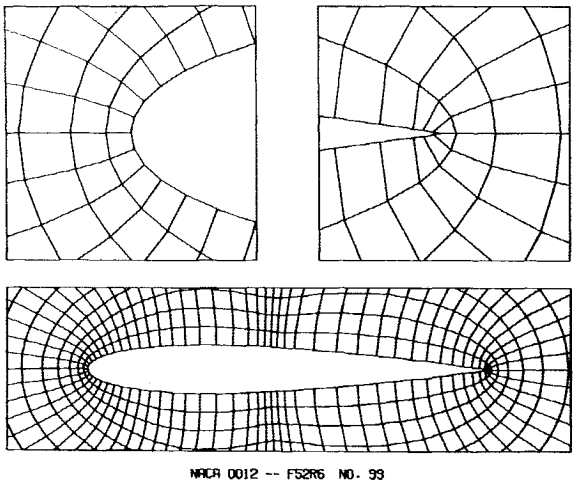

Fig. 8a Selected portions of grid 4.

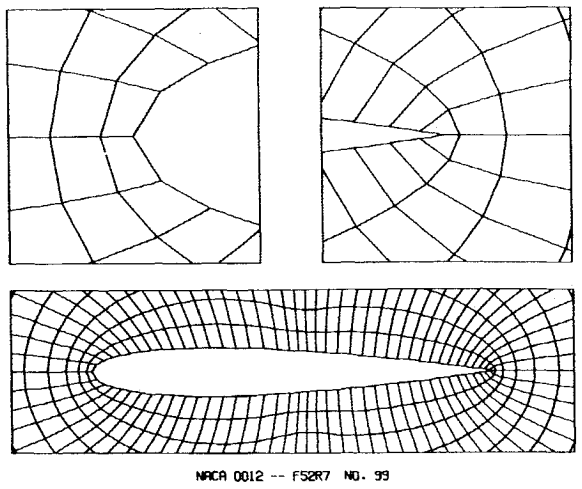

Fig. 9a Selected portions of grid 5.

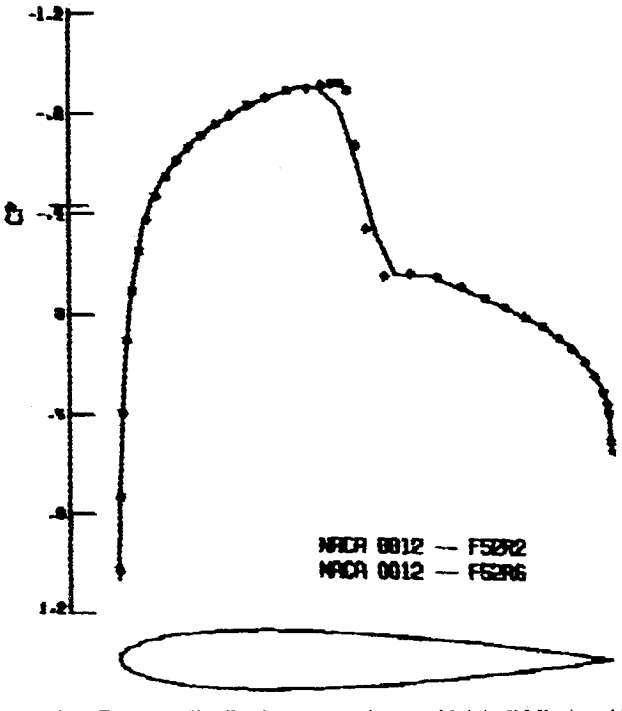

Fig. 8b Pressure distribution comparison: grid 1 (solid line), grid 4 (symbols).

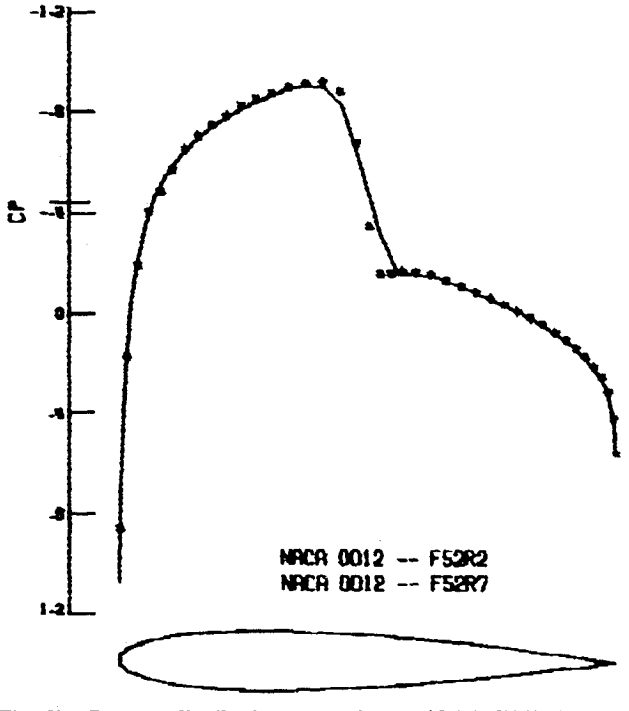

Fig. 9b Pressure distribution comparison: grid 1 (solid line), grid 5 (symbols).

Table 1, three methods were considered here. In the first (grid 3), points on the airfoil boundary were not allowed to move. In the second (grid 4), points were allowed to move to insure, to the highest degree possible, orthogonality on the airfoil boundary. The last scheme (grid 5) requires the point distribution on the boundary to be proportional to that on the first interior grid line. That is,

$$(s_i/s_{\max})_{\eta=1} = (s_i/s_{\max})_{\eta=2} \tag{15}$$

where s is the arc length, $\eta=1$ represents the airfoil surface, and $\eta=2$ signifies the initial interior grid line. Implementation of the second method is discussed in Appendix B.

The results of the calculations outlined above are shown in Figs. 7-9. Recall that the solid line represents the solution obtained by FL052 on its "own" grid (grid 1). Each of the figures illustrates details of the adaptive grid for $\beta_v=10$ and $\beta_0=0$ close to the airfoil and a comparison of the pressure distributions obtained by FL052 on grid 1 and one of the adaptive grids. In all of these cases, better resolution of the shock is indicated. Since the total number of points on the boundary remained fixed for all calculations, a coarser grid results around the leading and trailing edges when points on the boundary are permitted to move. In spite of this undesirable behavior, the calculated pressure distribution remains in good agreement with the FL052 solutions computed on grid 1 in these regions.

Concluding Remarks

A simple scaling procedure is incorporated into the Brackbill and Saltzman method for generating adaptive grids. It is shown that the procedure dictates certain forms of the weight function necessary for successful grid adaptation. Two problems representative of viscous and inviscid flows of current interest are considered. Based on our experience with the method, it is felt that variational methods, when coupled with proper scaling, are highly suited for generating adaptive grids.

It should be pointed out that the procedure presented here for generating adaptive grids is general and flexible so that it can be incorporated with little effort into other flow solvers.

The cost of grid adaptation depends on the frequency of generation of a new grid. In general, if one seeks a steady-state solution, then there is little to be gained from repeated grid generation.

Acknowledgments

This work has been supported in part by NASA Cooperative Agreement NCCI-22.

Appendix A: Grid Equations and Their Solutions

As a first step in deriving the Euler equations for the variational problem under consideration, the integrals defined by I_s, I_0, and I_v are transformed to the computational plane (ξ,η). Noting that[3]

$$\xi_x = y_\eta/J, \quad \xi_y = -x_\eta/J, \quad \eta_x = -y_\xi/J, \quad \eta_y = x_\xi/J \tag{A1}$$

the integrals under consideration can be represented as

$$I_\sigma = \iint F_\sigma \mathrm{d}\xi \mathrm{d}\eta, \qquad \sigma = s,0,v \tag{A2}$$

where

$$F_s = (x_\xi^2 + x_\eta^2 + y_\xi^2 + y_\eta^2)/J$$

$$F_0 = (x_\xi x_\eta + y_\xi y_\eta)^2$$

$$F_v = wJ^2 \tag{A3}$$

The desired Euler equations in two dimensions can be written as

$$\left(\frac{\partial}{\partial x}\frac{\partial}{\partial \xi}\frac{\partial}{\partial x_\xi} - \frac{\partial}{\partial \eta}\frac{\partial}{\partial x_\eta}\right)(\Sigma F_\sigma) = 0 \tag{A4}$$

$$\left(\frac{\partial}{\partial y}\frac{\partial}{\partial \xi}\frac{\partial}{\partial y_\xi} - \frac{\partial}{\partial \eta}\frac{\partial}{\partial y_\eta}\right)(\Sigma F_\sigma) = 0 \tag{A5}$$

Substitution of Eqs. (A3) into Eqs. (A4) and (A5) and carrying out the indicated operation, one finds that the grid equations take the form

$$b_1 x_{\xi\xi} + b_2 x_{\xi\eta} + b_3 x_{\eta\eta} + a_1 y_{\xi\xi} + a_2 y_{\xi\eta} + a_3 y_{\eta\eta} = d_1 \tag{A6}$$

$$a_1 x_{\xi\xi} + a_2 x_{\xi\eta} + a_3 x_{\eta\eta} + C_1 y_{\xi\xi} + C_2 y_{\xi\eta} + C_3 y_{\eta\eta} = d_2 \tag{A7}$$

where

$$a_k = a_{sk} + \lambda_0 a_{0k} + \lambda_v w a_{vk} \tag{A8}$$

$$b_k = b_{sk} + \lambda_0 b_{0k} + \lambda_v w b_{vk} \tag{A9}$$

$$c_k = c_{sk} + \lambda_0 c_{0k} + \lambda_v w c_{vk} \tag{A10}$$

with

$$a_{sk} = -A\alpha,\ 2A\beta,\ -A\gamma$$

$$b_{sk} = B\alpha,\ -2B\beta,\ B\gamma$$

$$c_{sk} = C\alpha,\ -2C\beta,\ C\gamma \tag{A11}$$

$$a_{0k} = x_\eta y_\eta,\ x_\xi y_\eta + x_\eta y_\xi,\ x_\xi y_\xi$$

$$b_{0k} = x_\eta^2,\ 2(2x_\xi x_\eta + y_\xi y_\eta),\ x_\xi^2$$

$$c_{0k} = y_\eta^2,\ 2(x_\xi x_\eta + 2y_\xi y_\eta),\ y_\xi^2 \tag{A12}$$

$$a_{vk} = -x_\eta y_\eta,\ x_\xi y_\eta + x_\eta y_\xi,\ -x_\xi y_\xi$$

$$b_{vk} = y_\eta^2,\ -2y_\xi y_\eta,\ y_\xi^2$$

$$c_{vk} = x_\eta^2,\ -2x_\xi x_\eta,\ x_\xi^2 \tag{A13}$$

$$d_1 = -\frac{J^2}{2}\frac{\partial w}{\partial x}\lambda_v, \quad d_2 = -\frac{J^2}{2}\frac{\partial w}{\partial y}\lambda_v \tag{A14}$$

$$A = x_\xi y_\xi + x_\eta y_\eta, \quad B = y_\xi^2 + y_\eta^2, \quad C = x_\xi^2 + x_\eta^2$$

$$\alpha = (x_\eta^2 + y_\eta^2)/J^3, \quad \beta = (x_\xi x_\eta + y_\xi y_\eta)/J^2$$

$$\gamma = (x_\xi^2 + y_\xi^2)/J^3 \tag{A15}$$

Before discussing a method of solution, Eqs. (A6) and (A7) are written as

$$(A_1 L_{\xi\xi} + A_2 L_{\xi\eta} + A_3 L_{\eta\eta})V = D \tag{A16}$$

where

$$D = d_1, d_2, \quad V = x, y, \quad L_{\xi\xi} = \partial^2/\partial\xi^2, \ldots \tag{A17}$$

and A_1, A_2, and A_3 are 2×2 matrices. Equation (A16) is solved by employing ADI or splitting techniques. The method employed here is that of Peaceman and Rachford.[10] Application of this method yields

$$[\rho_n I + A_1^n L_{\xi\xi} + A_2^n L_{\xi\eta} + A_3^n L_{\eta\eta}]\Delta V$$

$$= D - [A_1 L_{\xi\xi} + A_2 L_{\xi\eta} + A_3 L_{\eta\eta}]^n V \equiv R^n \tag{A18}$$

where ρ_n is a relaxation factor for the nth iteration. An algorithm based on Eq. (A18) was implemented using the two steps

$$[\rho_n I + A_1^n L_{\xi\xi}]\Delta V = R^n \tag{A19}$$

$$[\rho_n I + A_3^* L_{\eta\eta}]\Delta V^* = R^* \tag{A20}$$

with

$$\Delta V = V^* - V^n, \quad \Delta V^* = V^{n+1} - V^*, \quad R^* = R(V^*) \tag{A21}$$

Appendix B: Implementing the Orthogonality Boundary Condition

Since the interior grid is adapting to a specified criterion, we wish to "impress" or "extrapolate" the interior structure onto the boundary. One way to do this is to require the grid to be locally orthogonal at the boundary. A local normal is projected from each point along the $\eta = 2$ line onto the boundary, or $\eta = 1$ line. Use is then made of the fact that the distance L between any point on $\eta = 2$, such as $(i,2)$, and the boundary along the projected normal is minimum.

If $x(s)$, $y(s)$ represent a point on the boundary, where s is the arc length, then,

$$L^2 = (x_{i,2} - x(s))^2 + (y_{i,2} - y(s))^2 \tag{B1}$$

The s location that minimizes L is obtained by setting the derivative of L to zero, i.e.,

$$(x_{i,2} - x(s))\frac{\mathrm{d}x}{\mathrm{d}s} + (y_{i,2} - y(s))\frac{\mathrm{d}y}{\mathrm{d}s} = 0 \tag{B2}$$

Equation (B2) is an equation for s that can be solved by Newton's method.

The above procedure does not work in the trailing-edge region of the airfoil. For such a region, an adaptation of the scheme given by Eq. (15) may be used.

References

[1]Anderson, D. A., "Adaptive Grid Methods for Partial Differentiation Equations," *Advances in Grid Generation*, ASME Fluids Engineering Conference, Houston, TX, 1983.

[2]Thompson, J. F., "A Survey of Dynamically Adaptive Grids in the Numerical Solution of Partial Differential Equations," AIAA Paper 84-1606, 1984.

[3]Brackbill, J. U. and Saltzman, J. S., "Adaptive Zoning for Singular Problems in Two Dimensions," *Journal of Computational Physics*, Vol. 46, 1982, pp. 342-368.

[4]Dwoyer, D. L. and Thames, F. C., "Accuracy and Stability of Time-Split Difference Schemes," AIAA Paper 81-1005, 1981.

[5]Jameson, A., Schmidt, W., and Turkel, E., "Numerical Solutions of the Euler Equations by Finite Volume Methods Using Runge-Kutta Time-Stepping Schemes," AIAA Paper 81-1259, 1981.

[6]Nakamura, S., "Adaptive Grid Relocation Algorithms for Transonic Full Potential Calculations Using One-Dimensional or Two-Dimensional Diffusion Equations," *Advances in Grid Generation*, ASME Fluids Engineering Conference, Houston, TX, 1983.

[7]Steinbrenner, J. P., Tassa, Y., and Anderson, D. A., "An Adaptive Grid Scheme Applied to Two-Dimensional Airfoil Problems," AIAA Paper 84-1608, 1984.

[8]Dwyer, H. A., "Grid Adaptation for Problems with Separation, Cell Reynolds Number, Shock-Boundary Layer Interaction, and Accuracy," AIAA Paper 83-0449, 1983.

[9]Gnoffo, P. A., "A Vectorized Finite-Volume, Adaptive-Grid Algorithm Applied to Planetary Entry Problems," AIAA Paper 82-1018, 1982.

[10]Peaceman, D. W. and Rachford, H. H. Jr., "The Numerical Solution of Parabolic and Elliptic Differential Equations," *Journal of the Society of Industrial and Applied Mathematics*, Vol. 3, March 1955, pp. 28-41.